Hot Corrosion Studies of Plasma-sprayed MWCNTs- Al_2O_3 Composite Coatings in Molten Salt Environment at 900°C

Rakesh Goyal[a,*], Buta Singh Sidhu[b], Vikas Chawla[c]

[a] *Chitkara University Institute of Engineering and Technology, Chitkara University, India*
[b] *Department of Mechanical Engineering, MRS Punjab Technical University, Bathinda, Punjab, India*
[c] *Department of Mechanical Engineering, IKG Punjab Technical University, Kapurthala, Punjab, India*

Abstract

This research work enquires the hot corrosion behavior of plasma coated boiler steel in the salt environment under cyclic conditions. The coating was carried out by alumina and CNT reinforced alumina composite powders. The substrates were tested in a tube furnace at 900°C. After exposure, thermogravimetric analysis was carried out with XRD, SEM, and EDS analysis to appraise the corrosion phenomenon. The present research concludes that CNT reinforced alumina coatings provide better corrosion resistance.

Keywords: Thermal spray coating, Plasma Spraying, Molten Salt Corrosion, Carbon nanotubes, Corrosion Protection.

1. Introduction

At elevated temperature, the surfaces of metals and alloys are covered with a film of deposited salt, and this is called hot corrosion [1]. Advancements in material development and cooling technologies have caused increase in temperature of turbines and industrial boilers [2]. The low grade coal usage in boilers requires specific attention to this type of hot corrosion. The impurities like S, Na, V and K are present in fuel. These impurities form compounds which melt at low temperature and get deposited on material and subsequently cause corrosion. These impurities react with themselves to form Na_2SO_4, V_2O_5 and vanadates [3]. These compounds are called ash. The ash destroys the naturally formed oxide layers on the materials at high temperature and hence accelerates the corrosion rate [1]. Plasma spraying is a versatile and well settled procedure to spray coatings for improved corrosion resistance on components of boiler [3]. This process is helpful to deposit ceramics as well as metals and metals-ceramics composites [4]. Plasma coatings of many type of materials such as alumina, zirconia and other similar materials have been developed [5]. Alumina having high hardness, chemically stable with high melt-point is able to maintain strength at 1100°C. It is studied from the literature that corrosion resistance of alumina coating is greater than other types of coatings [6]. One of the limitations of these coatings is the cracks and corrosion of metals through these cracks. Therefore, the corrosion resistance of such coatings may further be improved [7]. Carbon nanotubes (CNTs) were invented in 1990s. These are 100's of times stronger than all types of steels and are having very high thermal and electrical properties [8]. The important attributes of CNTs make these suitable reinforcement material for composites [9]. Some investigators have increased the corrosion resistance of CNTs mixed composite coatings. A few investigators have evaluated the tribological properties of CNTs-alumina composite coatings [10]. But no investigation on CNTs-alumina composite coatings for hot corrosion of steels are present. So, there is scope of evaluating hot corrosion behavior of CNTs-alumina mixed coatings on boiler steels in molten salt environment. The authors are presenting this research work in continuation of his previous publications [11, 12] on plasma sprayed CNT mixed alumina coatings. In this research work, hot corrosion behaviour of plasma sprayed alumina and CNT mixed alumina coatings deposited on T11 boiler steel are studied in molten salt environment. The results are then supported by various testing techniques like metallography, SEM, EDS and XRD.

2. Experimental Details

2.1. Substrate Material, Development and Characterization of Coatings

As the boiler steel selected for the investigation was Grade T11. This steel has been widely used in various power plants boilers of North India. After procuring this steel in tube form, the tube was cut into 20 mm × 15 mm × 5 mm rectangular sized samples for testing. These rectangular samples, were polished on all the six faces, as per standard metallurgical procedure down to 220 grit size. The chemical composition of the steel was examined

*Corresponding Author
Email address: rakesh.goyal@chitkara.edu.in (Rakesh Goyal)

at the CIDCO-IDFC testing laboratory, Chandigarh, and the result is reported in Table 1. Different compositions

Table 1: Chemical composition (wt.%) of Grade T11 boiler steel

ASME code	Composition	C	Mn	Si	S	P
SA213-T-11	Nominal	0.15	0.3-0.6	0.5-1	0.03	0.03
	Actual	0.1911	0.628	0.338	0.0128	0.0136
	Composition	Cr	Mo	V	Ni	Fe
	Nominal	1-1.5	0.44-0.65	-	-	Bal.
	Actual	1.064	0.01	0.0217	0.517	Bal.

of coating powders were prepared by blending alumina (size 40 ± 10 μm; minimum assay 99 %, Spraymet, Karnataka, India) with 1.5, 2, and 4 wt.% multiwalled carbon nanotubes (size ; Outer Diameter ± Length = 6-9 nm ± 5 μm; minimum assay 95%, Sigma-Aldrich Chemicals, USA) in a laboratory ball mill, using low-energy ball milling method. All the six sides of the sample were coated. Firstly, Ni-Cr powder (Powder Alloy Coppn, Ohio, USA) has been deposited as bond coat, then the coatings were deposited on the substrates at Anod Plasma Ltd. Kanpur, India. The composition details and designation of coating powders is reported in Table 2. The process parameters were tested and optimized before spraying. The deposition parameters are summarized in Table 3. The literature related to

Table 2: Chemical composition and designation of coating powders

S. No.	Designation of coating	Chemical composition, wt.%
1.	0CAl2O3	Al2O3
2.	1.5CAl2O3	1.5% CNT- 98.5% Al2O3
3.	2CAl2O3	2% CNT-98% Al2O3
4.	4CAl2O3	4% CNT- 96% Al2O3

Table 3: The process parameters used during plasma spraying

Spray Parameters	Bond Coat	Alumina
Arc Current (A)/Voltage (V)	550/50	550/50
Argon pressure (psi)	60	60
Hydrogen pressure (psi)	10	10
Spraying Distance (mm)	90-110	90-110
Hopper RPM	6.5	1.5
Powder Gas Pressure (psi)	50	45

characterization of these coating has been published elsewhere by the same authors [12]. The thickness range of coatings comes out to be as 200±10 μm, as measured from BSE - cross-sectional micrographs. The porosity of coatings was measured with the help of 'LEICA Image analyzer' (Germany made). The porosity of Al_2O_3 coated specimen was determined to be higher than 4%, but the porosity was found to be less than 4% with the increase of CNTs in Al_2O_3. The adhesion strength of the CNTs mixed coatings was noticed to be increased with the increase in CNTs content. For $4CAl_2O_3$ coatings, it was measured as 17.6 MPa, whereas for $0CAl_2O_3$ it was 11.7 MPa. The CNTs were noticed to be uniformly present in the Al_2O_3 matrix is shown in the as sprayed and inset image Fig.1 (a-b). CNTs have been chemically stable during the spray process. There was not any formation of carbides as well as oxides regardless of the high temperature.

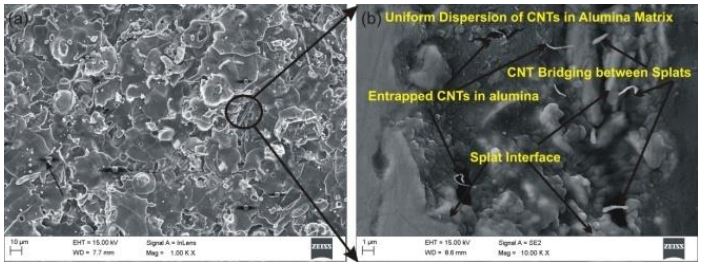

Figure 1: SEM micrograph for plasma-spray coated boiler steel (a) as-sprayed and (b) Inset SEM showing CNTs in alumina splats.

2.2. Hot Corrosion Studies in Molten Salt ($Na_2SO_4 - 60\%V_2O_5$)

Hot corrosion study in molten salt environment was carried at 900 ˚C in a laboratory silicon carbide (SiC) tube furnace. A platinum-rhodium thermocouple was used to calibrate the furnace temperature to an accuracy of ±5 ˚C. The specimens were polished with 1 μm alumina wheel cloth to get the similar surfaces before being exposed to corrosion study. The dimensions (length, breadth, thickness) of each specimen were measured before performing studies. Then, the samples were acetone washed and after dried in hot air so as to remove the moisture. Each sample was placed in an alumina boat. After the collective weight of sample and boat was measured. The boats were pre heated at 1200 ˚C for 6 hours. The specimens were then heated up to 250 ˚C. A mixture of ($Na_2SO_4 - 60\%V_2O_5$ and distilled water was prepared in a glass vessel. Camel hair brush was used to apply this salt mixture on the warm polished samples. The amount of this salt coating was maintained in the range of 3.0-5.0 mg/cm^2. The samples and the boats were then dried in an oven for 3-4 hrs. at 100 ˚C and weight is noted before the start of hot corrosion testing. The samples after application of salt coating were subjected to laboratory furnace at 900 ˚C for 50 cycles. The 50 cycles study was selected for experimentations, because this is considered to be an effective steady state of hot corrosion for boiler steels. The samples were heated for one hour in furnace, and then cooled for 20 minutes at ambient temperature. The sample and boat was collectively weighted after each

cycle with electronic balance. The scale which was spalled from the sample, in the boat, during testing was also considered into measurement for the weight change. The cyclic load was used to create the actual cyclic conditions for experiments, because the cyclic conditions provide a real approach for problems of high-temperature corrosion in actual industrial environment.

3. Results

3.1. Visual Examination

After every cycle, each sample was examined visually for variation in colour, luster and development of cracks in the oxide scales. The macrographs for all T11 steel samples (uncoated and coated) after experimentation are presented in Fig.2 (a-e). For uncoated T11 steel dark

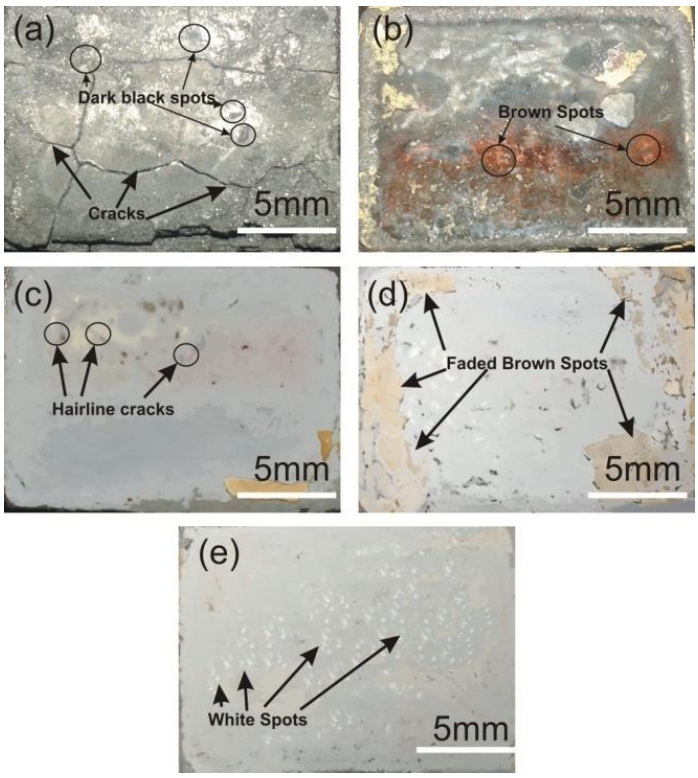

Figure 2: Surface macrograph of: (a) Uncoated T11, (b) 0CAl_2O_3 coating, (c) 1.5CAl_2O_3 coating, (d) 2CAl_2O_3 coating, (e) 4CAl_2O_3 coating after hot corrosion

black shining spots were noticed on the surface after 2^{nd} cycle. The scale was lustrous and started cracking during the 22^{nd} cycle. The cracks grow further which leads to falling of the scale in the boat. Spalling and wider cracks were observed in the remaining cycles. When the subscale is formed, the top layer splits and the isolated different layers covering each other were viewed as appear in Fig.2 (a). For 0CAl_2O_3 coated T11 as indicated in Fig.2 (b), the cracks appeared in the coating after 17^{th} cycle, and after 50 cycles it was found that some part of the coating was spalled off and brownish spots are clearly seen upon the surface of substrate due to hot corrosion. The Fig.2 (c) reveals the macrograph of 1.5CAl_2O_3 coated T11 steel. Some hairline cracks in the coating appeared after 27^{th} cycle and continued till 50 cycles. The Fig.2 (d) shows the macrograph of 2CAl_2O_3 coated T11 steel, showed no sign of spalling in the initial cycles. Although the colour of the scale has been changed to faded brown at some points. After 29^{th} cycle hairline cracks were observed along the edges but the scale is adherent till 50^{th} cycle. In case of 4CAl_2O_3 coated T11 steel (Fig.2 (e)), no spalling has been noticed till 50 cycles. Few white spots on surface of scale can be seen. The coating was found intact, without any signs of cracks after the completion of 50 cycles.

3.2. Weight Change Data

The plots for weight gain/ unit area (mg/cm^2) versus time expressed in number of cycles for uncoated and coated T11 steel are shown in Fig.3. The plots for all the samples show high weight gain during initial cycles followed. After the weight gain took place gradually. It is clear from the plots that uncoated T11 steels have shown higher corrosion in comparison to the coatings. Conventional Al_2O_3 coating too has decreased the weight gain. CNTs mixed Al_2O_3 coatings has shown lesser weight gain in comparison to uncoated and 0CAl_2O_3 coated T11 steel. Figure4 shows

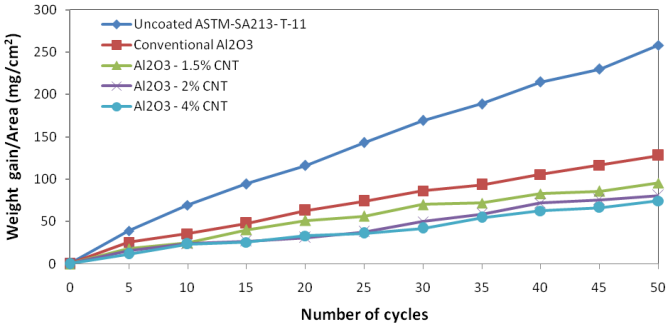

Figure 3: Weight gain/area vs. time (number of cycles) for all specimens after hot corrosion.

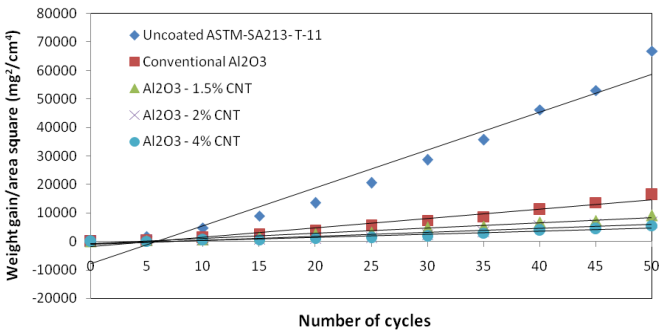

Figure 4: (Weight gain/area)^2 vs. time (number of cycles) for all specimens after hot corrosion.

the plots of (weight gain/area)^2 versus number of cycles for all coatings depicts that all coatings have approximately obeyed parabolic rate law. The parabolic rate constant K_p was with the formula $(W/A)^2 = K_p$ t, where W/A is the weight change per unit surface area (mg/cm^2) and "t" is number of cycles of experiment. The parabolic rate

Table 4: Parabolic rate constant (K_p) for specimens

Description	Kp values (10-10g2 cm-4s-1)	Total weight gain (mg/cm2)
Uncoated T11 steel	3741.67	258.47
0CAl2O3	908.05	127.91
1.5CAl2O3	515.27	95.66
2CAl2O3	378.88	80.83
4CAl2O3	306.94	74.36

constants are shown in Table 4. It is inferred that the 'K_p' values for the CNTs-Al_2O_3 coated T11 steel were less than that of uncoated, and 0CAl_2O_3 coated T11 steel.

3.3. X-ray Diffraction Analysis

X-ray peaks for uncoated, 0CAl_2O_3, 1.5CAl_2O_3, 2CAl_2O_3 and 4CAl_2O_3 coated steels after cyclic corrosion testing is given in Fig.5 (a-e). The formation of oxides of Fe could be identified in case of bare steel. The prominent phase noticed for this steel is Fe_2O_3. Al_2O_3 was noticed as the major phase formed in the 0CAl_2O_3 coated T11 steel after exposure to the molten salt surroundings (Fig.5 (b)). Minor peaks of NiO, Na_2SO_4, Cr_2O_3 and Fe_2O_3 phases has also been detected. In the caseof1.5CAl_2O_3, 2CAl_2O_3 and 4CAl_2O_3 coated T11 steels (Fig.5 (c-e)), Al_2O_3 was detected as the main phase and carbon, Na_2SO_4 and V_2O_5 has been observed as the minor XRD phases.

3.4. EDS Analysis

FE-SEM and EDS analysis for uncoated as well as coated T11 steel samples after testing is presented in Fig.6. The surface morphology of uncoated steel (Fig.6 (a)) indicated irregular flakes with random orientation. The scale appears to be porous. In EDS analysis of uncoated steel at points 1 and 2 in the micrograph, it was noted that the scales are concentrated with O and Fe and a small amount of elements such as Na and V was also observed. The presence of O and Fe confirmed the formation of Fe_2O_3 phase, which were noted in XRD analysis of the same substrates. Figure6 (b) shows surface morphology of 0CAl_2O_3 coated specimen as thick irregular flake scales. In EDS analysis of 0CAl_2O_3 coated T11 steel exposed to molten salt environment, it was noted that the scale was rich in Al, O and Fe elements and some amount of Na, Ni, and Cr elements also found. These elements leaded to the formation of Al_2O_3, Fe_2O_3, Na_2SO_4, Cr_2O_3 and NiO phases. The micrograph of

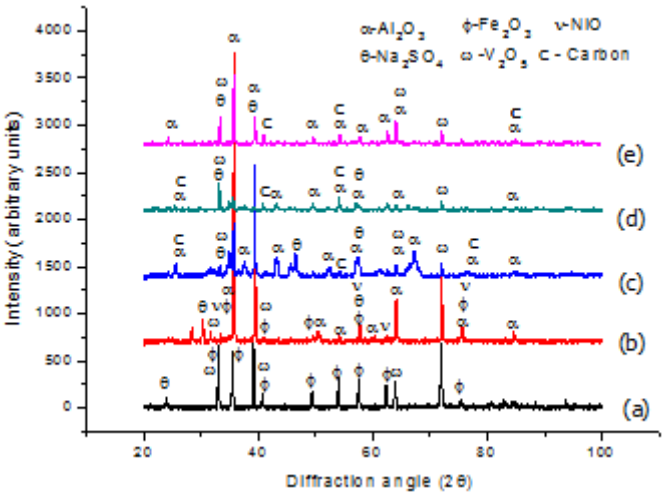

Figure 5: (XRD peaks of (a) Uncoated T11, (b) 0CAl_2O_3 coating, (c) 1.5CAl_2O_3 coating, (d) 2CAl_2O_3 coating, (e) 4CAl_2O_3 coating after hot corrosion.

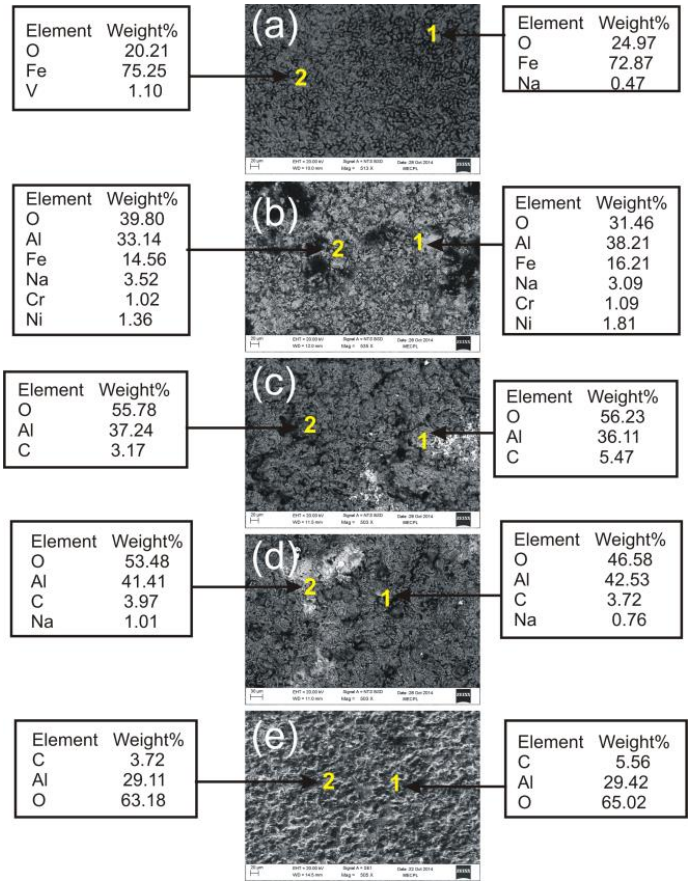

Figure 6: FE-SEM and EDS analysis of: (a) Uncoated T11, (b) 0CAl_2O_3 coating, (c) 1.5CAl_2O_3 coating, (d) 2CAl_2O_3 coating, (e) 4CAl_2O_3 coating after hot corrosion.

1.5CAl_2O_3 coatedT11 steel (Fig. 6 (c)) showed dense granular scale. In EDS analysis, at points 1 and 2, of the same substrate, it was noted that the along with Al and

O in composition and there is a minor percentage of C in the scale. Figure6 (d) shows surface morphology of 2CAl_2O_3 coated T11 steel substrate after experimentation. In EDS analysis of the same substrate, at points 1 and 2, it was noted that the major elements present in the scale were O and Al there is a minor percentage of C and Na in the scale. The surface morphology of 4CAl_2O_3 coated T11 steel substrate exposed to the molten salt environment (Fig.6 (e)) shows dense regular scales. The EDS analysis of the same substrate at point 1 and 2 in the micrograph showed the top scale is rich in Al and O elements and C element is present in a minor amount. The noted elements formed the phases such as Al_2O_3 and of C. The same has been observed from the XRD analysis of same substrate.

3.5. Cross-sectional Analysis

SEM Micrographs and elemental variation throughout the cross-section of all specimens are given in Fig.7 (a-e). SEM micrograph of the uncoated T11 steel in Fig.7 (a) shows cracks and dark spots in the scale with the significant amount of corrosion. The oxygen is present in the significant amount throughout the scale (point 2 to 6). Therefore, there seems a tendency of Fe_2O_3 in the oxide scale. Figure 7 (b) shows micrograph of the plasma-sprayed 0CAl_2O_3 coated T11 steel after exposure. Continuous adherent scale with cracks at many locations was noticed. The presence of Al, Fe, and O (point 3 to 6) in scale clearly signals the presence of oxides of aluminium and iron. The presence of Ni and Cr can also be noticed in the scale near the interface (point 2). The micrograph for the cross-section (Fig.7 (c)) for 1.5CAl_2O_3 coating indicates that the scale is adherent to the substrate. The C can be seen in major proportion at points 4 to 7 representing the CNTs in the coating matrix. SEM micrographs and variations in elemental composition for 2CAl_2O_3 and 4CAl_2O_3 coated T11 steels are shown in Fig.7 (d- f). The significant amount of C is present in the scale (point 4 to 7) owing to the presence of CNTs in the alumina matrix. The coating layer is intact.

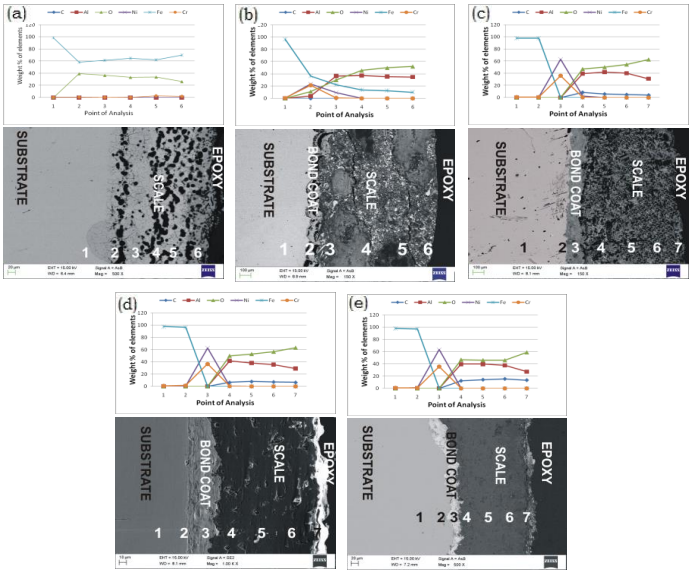

Figure 7: SEM micrograph and elemental variation across the cross-section of (a) Uncoated T11 steel, (b) 0CAl_2O_3 coating, (c) 1.5CAl_2O_3 coating, (d) 2CAl_2O_3 coating, (e) 4CAl_2O_3 coating after hot corrosion.

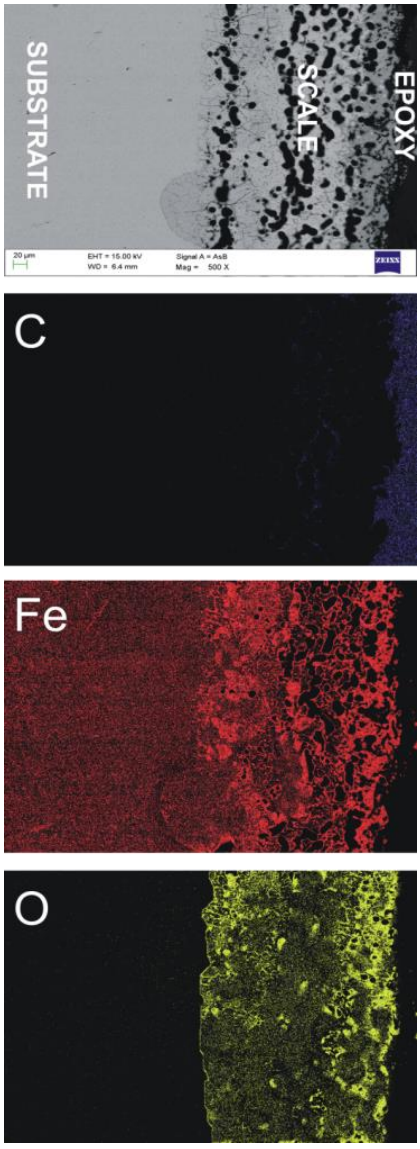

Figure 8: Composition image and X-ray mappings across the cross-section of the T11boiler steel after hot corrosion.

3.6. X-ray Mapping Analysis

X-ray mappings for a section of oxide scale of all specimens are shown in Figs. 8- 12. The micrograph of bare hot corroded steel showed in Fig. 8, signals the significant corrosion along the scale-substrate interface

and results in the formation of oxide scale which is mainly composed of iron oxide. The O has been seen penetrated deep into the substrate, as pointed by X-ray mapping. Compositional image and X-ray mapping of the 0CAl_2O_3 coated T11 steel after exposure is presented in Fig.9. The mapping signals the presence of Al, Fe, and O throughout the scale along with Ni, and Cr near the interface.

Compositional images for CNT-Al_2O_3 coated T11 steels subjected to cyclic testing are showed in Fig. 10 - 12. The X-ray mapping signals the presence of Al, O along with minor traces of C throughout the scale. The traces of C becomes more significant, with the increase of CNTs in the composite coating. The X-ray mappings indicates that the interface between coating and substrate is plentiful in Ni, and Cr. This evinces the presence of bond coat at the interface.

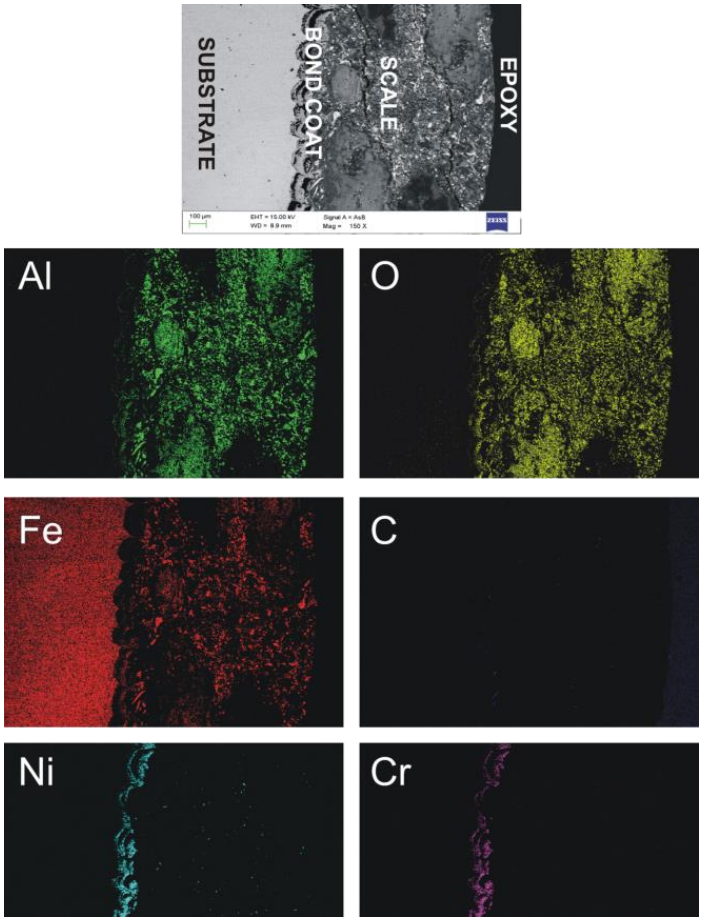

Figure 9: Composition image and X-ray mappings across the cross-section of the 0CAl_2O_3 coated T11 boiler steel after hot corrosion.

4. Discussion

The uncoated T11 type of steel after cyclic hot corrosion study in the molten salt environment at 900 °C has indicated parabolic behaviour. In the salt environment, the corrosion resistance of T11 steel is lesser

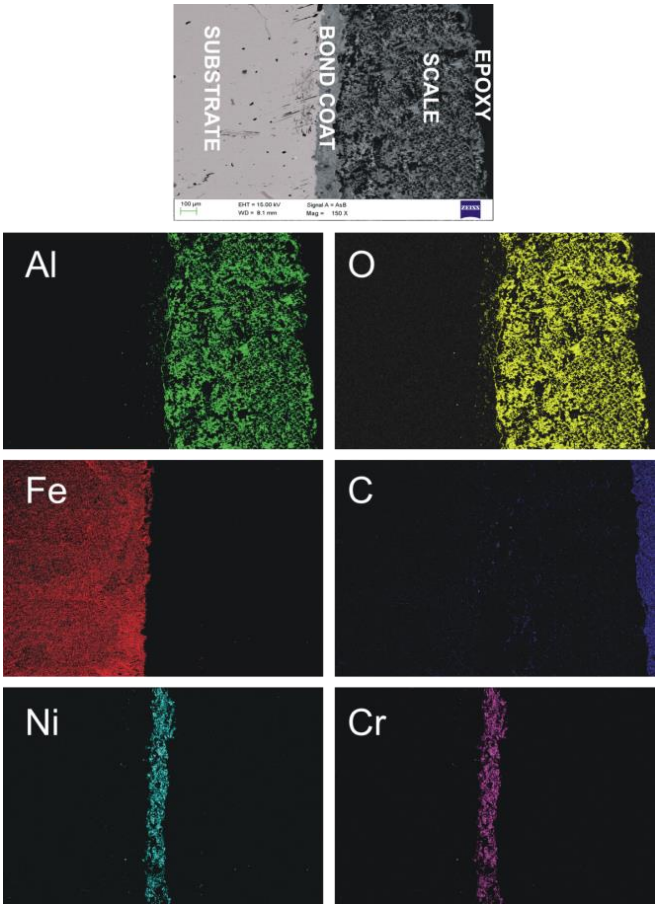

Figure 10: Composition image and X-ray mappings across the cross-section of the 1.5CAl_2O_3T11 boiler steel after hot corrosion.

than that in air due to presence of V, Na and S [13]. High spalling and higher corrosion rate was noticed for this bare steel. Parabolic rate constant (K_p value) of this type of steel is $37.41\pm10^{-8} g^2 cm^{-4} s^{-1}$. The identification of Fe_2O_3 by XRD and EDS analysis in the scales of the bare T11 steel shows that non protective environment was generated when Na_2SO_4-60%V_2O_5 salt was applied on specimen. Das *et al.* [14] also reported the formation of non protective Fe_2O_3 scale. Spalling and peeling of scale of bare T11 might be due to presence of Mo oxides [15]. The high corrosion during the starting cycles of the study might be because of oxygen diffusion as also reported by Sidhu and Prakash [16]. Hot corrosion of 0CAl_2O_3 coated T11 steel in molten salt is intense. Spalling may be one of the main causes for increase in corrosion. For this coated T11 steel, scale was regularly spalling; XRD peaks for the spalled scale showed the presence of Al_2O_3 with Fe_2O_3 constituents. Spalling might be initiated by the fast development of void-like imperfections which lie near to coating protuberances [17]. The tensile stress was appeared during cooling because of the thermal contraction difference of oxide and coating. The development of cracks may be initiated from stresses appeared in the salt deposits [18]. The corroding species

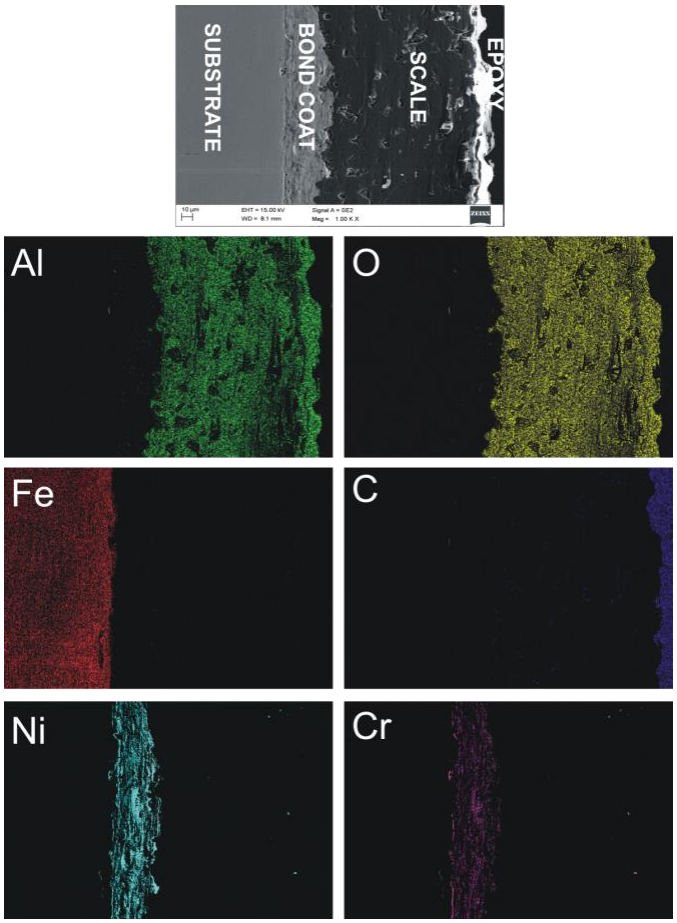

Figure 11: Composition image and X-ray mappings across the cross-section of the 2CAl_2O_3 T11 boiler steel after hot corrosion.

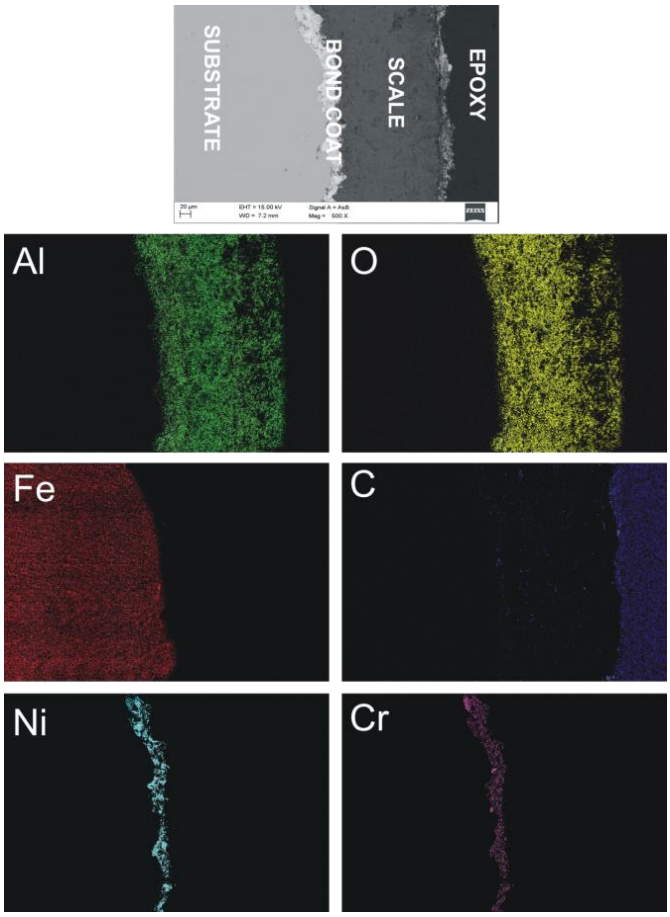

Figure 12: Composition image and X-ray mappings across the cross-section of the 4CAl_2O_3T11 boiler steel after hot corrosion.

may fastly penetrate to the base metal through the cracks and reduces its path through the coating which cause adhesion loss and spalling. Crack formation in the coating and further corrosion of base metal has also been revealed by Wang [19] for the alumina coating on alloy steel. The indication of Al_2O_3 in the surface scale, followed by the formation of Fe_2O_3 as analysed by XRD and EDS investigations may be because of the penetration of iron through voids and cracks which formed in the coatings. During investigation, an outer scale of NiO was also observed. This might be because of dispersion of Ni from the Ni-20Cr bond coat. This type of layer was reported to be loose by Wu et al. [20] and was not in corrosion prevention. Niranatlumpong *et al.* [17] proposed increment in pore sizes of Ni and Cr scales with increment in exposure time, which enables corrosive elements to diffuse subsequently bringing about the oxidation of substrate steels. Weight gain graphs indicate that the CNT-Al_2O_3 coatings has provided necessary protection. 4CAl_2O_3 coated T11 steel is the most effective among all the coatings. The weight gain value of this 4CAl_2O_3 coated T11 steel is only around 28% of that for uncoated steel. The order of hot corrosion in terms of weight gain for different CNT- Al_2O_3 coated steels is given as: T11 > 0CAl_2O_3> 1.5CAl_2O_3> 2CAl_2O_3> 4CAl_2O_3 Comparatively lesser weight gain values for CNT- Al_2O_3 coated steels can be due to presence of CNTs in the alumina. The XRD analysis revealed the peaks of Al_2O_3 along with C and are consistent with the peaks observed by Ahmad *et al.* [10]. Surface EDS of CNT- Al_2O_3 coated T11 steel indicated the presence of aluminium oxide and CNTs. Cross-sectional EDS analysis showed a very thin spinel of nickel and chromium at points 2 and 3 indicated the layer of bond coat at the interface of substrate and coating. The results of XRD and EDS analysis are further confirmed with elemental X-ray maps. Porosity of Al_2O_3 coating was also reduced because of CNTs reinforcement. Generally, the size of pores and holes on the surface of coatings is higher than submicron. Therefore, CNTs of the size lesser than 100 nm can enter and fill the pores, and thus reduce the porosity of coating. Dense coating is having better corrosion resistance than that of porous coatings. In this experimentation work, the CNTs were embedded deeply in the alumina grains. Thus reinforcement of CNTs in the Al_2O_3 coating matrix caused increased corrosion resistance. Similar observations has been made by Chen et al. [21] during his studies on the CNT-composite

coatings in corrosive environment.

5. Conclusion

In this work, the hot corrosion behaviour of uncoated T11 steel, conventional Al_2O_3 coated T11, 1.5, 2, and 4 wt.% CNTs-Al_2O_3 coated T11 was investigated at 900 °C in molten salt environment. The following conclusions are drawn:

1. The uncoated T11 steel indicated severe corrosion.
2. The CNT-Al_2O_3 coated boiler steels showed low weight gain in comparison to other coatings.
3. Coatings were proved to be helpful in enhancing the resistance to hot corrosion in following order: $4CA1_2O_3 > 2CA1_2O_3 > 1.5CA1_2O_3 > 0CA1_2O_3$
4. The XRD, SEM and EDS analysis of the corroded uncoated boiler steel specimens confirmed the presence of Fe_2O_3 phase after exposure. This oxide is fragile and non-protective. In case of Al_2O_3 coated boiler steel specimens; the presence of Al_2O_3 phase along with Fe_2O_3 was identified. Presence of Al_2O_3 improves the better performance of coating when compared to the uncoated steels.
5. The addition of CNTs results in interlocking of particles with regular morphology. The CNTs were properly mixed in alumina powder, and a proper bonding has taken place, which has resulted denser coatings.
6. The better performance of 4CAl_2O_3 coating than 0CAl_2O_3,1.5CAl_2O_3 and 2CAl_2O_3 coatings might be due to the presence of CNTs in the coating mixture.
7. 4CAl_2O_3 coating has indicated superior resistance to hot corrosion in molten salt environment of cyclic study. XRD analysis has indicated the presence of Al_2O_3 and C for this coating. The nano tubes of carbon of diameter lesser than 10 nm are easily embedded profoundly in the grains of Al_2O_3, and filled in cracks, and micron sized holes. These carbon nanotubes behave as blockages to the origination and growth of defect corrosion, improving the microstructure of the alumina layer and therefore improve the resistance to hot corrosion.

References

[1] T. Sidhu, S. Prakash, R. Agrawal, Hot corrosion and performance of nickel-based coatings, Current Science (2006) 41–47.

[2] S. Kamal, R. Jayaganthan, S. Prakash, Hot corrosion studies of detonation-gun-sprayed nicraly+ 0.4 wt.% ceo2 coated superalloys in molten salt environment, Journal of materials engineering and performance 20 (6) (2011) 1068–1077.

[3] X. Zhang, X. Jie, L. Zhang, S. Luo, Q. Zheng, Improving the high-temperature oxidation resistance of h13 steel by laser cladding with a wc/co-cr alloy coating, Anti-Corrosion Methods and Materials 63 (3) (2016) 171–176.

[4] B. S. Sidhu, D. Puri, S. Prakash, Mechanical and metallurgical properties of plasma sprayed and laser remelted ni–20cr and stellite-6 coatings, Journal of Materials Processing Technology 159 (3) (2005) 347–355.

[5] A. N. Khan, J. Lu, Thermal cyclic behavior of air plasma sprayed thermal barrier coatings sprayed on stainless steel substrates, Surface and Coatings Technology 201 (8) (2007) 4653–4658.

[6] E. Celik, I. Ozdemir, E. Avci, Y. Tsunekawa, Corrosion behaviour of plasma sprayed coatings, surface and coatings technology 193 (1-3) (2005) 297–302.

[7] V. P. Singh Sidhu, K. Goyal, R. Goyal, Corrosion behaviour of hvof sprayed coatings on asme sa213 t22 boiler steel in an actual boiler environment, in: Advanced Engineering Forum, Vol. 20, Trans Tech Publ, 2017, pp. 1–9.

[8] S. Iijima, Helical microtubules of graphitic carbon, nature 354 (6348) (1991) 56.

[9] M. K. Singla, H. Singh, V. Chawla, Thermal sprayed cnt reinforced nanocomposite coatings–a review, Journal of Minerals and Materials Characterization and Engineering 10 (08) (2011) 717.

[10] I. Ahmad, M. Unwin, H. Cao, H. Chen, H. Zhao, A. Kennedy, Y. Zhu, Multi-walled carbon nanotubes reinforced al2o3 nanocomposites: mechanical properties and interfacial investigations, Composites Science and Technology 70 (8) (2010) 1199–1206.

[11] R. Goyal, B. S. Sidhu, V. Chawla, Improving the high-temperature oxidation resistance of asme-sa213-t11 boiler tube steel by plasma spraying with cnt-reinforced alumina coatings, Anti-Corrosion Methods and Materials 65 (2) (2018) 217–223.

[12] R. Goyal, B. S. Sidhu, V. Chawla, Characterization of plasma-sprayed carbon nanotube (cnt)-reinforced alumina coatings on asme-sa213-t11 boiler tube steel, The International Journal of Advanced Manufacturing Technology 92 (9-12) (2017) 3225–3235.

[13] L. Paul, R. Seeley, Oil ash corrosion -a review of utility boiler experience, Corrosion 47 (2) (1991) 152–159.

[14] D. Das, R. Balasubramaniam, M. Mungole, Hot corrosion of carbon-alloyed fe3al-based iron aluminides, Materials Science and Engineering: A 338 (1-2) (2002) 24–32.

[15] F. Pettit, J. Goebel, G. Goward, Thermodynamic analysis of the simultaneous attack of some metals and alloys by two oxidants, Corrosion Science 9 (12) (1969) 903–913.

[16] B. S. Sidhu, S. Prakash, Evaluation of the corrosion behaviour of plasma-sprayed ni3al coatings on steel in oxidation and molten salt environments at 900 c, Surface and Coatings Technology 166 (1) (2003) 89–100.

[17] P. Niranatlumpong, C. Ponton, H. Evans, The failure of protective oxides on plasma-sprayed nicraly overlay coatings, Oxidation of Metals 53 (3-4) (2000) 241–258.

[18] G. Heath, P. Heimgartner, G. Irons, R. D. Miller, S. Gustafsson, An assessment of thermal spray coating technologies for high temperature corrosion protection, in: Materials science forum, Vol. 251, Trans Tech Publ, 1997, pp. 809–816.

[19] D. Wang, Corrosion behavior of chromized and/or aluminized 214cr-1mo steel in medium-btu coal gasifier environments, Surface and Coatings Technology 36 (1-2) (1988) 49–60.

[20] X. Wu, D. Weng, Z. Chen, L. Xu, Effects of plasma-sprayed nicral/zro2 intermediate on the combination ability of coatings, Surface and Coatings Technology 140 (3) (2001) 231–237.

[21] X. Chen, C. Chen, H. Xiao, F. Cheng, G. Zhang, G. Yi, Corrosion behavior of carbon nanotubes–ni composite coating, Surface and Coatings Technology 191 (2-3) (2005) 351–356.